

Supporting Information

Solvent- and anion-controlled photochromism of viologen-based metal-organic hybrid materials

Jian-Ke Sun,^{ac} Peng Wang,^{ac} Qing-Xia Yao,^a Yong-Juan Chen,^b Zhao-Hui Li,^b
Yong-Fan Zhang,^b Li-Ming Wu^a and Jie Zhang^{*a}

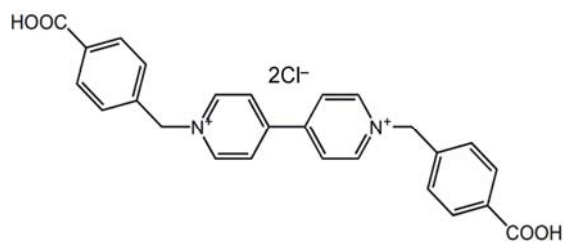
^a State Key Laboratory of Structural Chemistry, Fujian Institute of Research on the Structure of Matter, Chinese Academy of Sciences, Fuzhou, Fujian 350002, P. R. China. E-mail: zhangjie@fjirsm.ac.cn; Fax: (+86) 591-83710051

^b College of Chemistry and Chemical Engineering, Fuzhou University, Fuzhou, Fujian 350002, P. R. China

^c Graduate School of Chinese Academy of Sciences, Beijing, 100039, P. R. China

Additional characterization data and figures

- Scheme 1** The structural scheme of H₂BpybcCl₂
- Fig. S1** Total and partial density of states for **1**.
- Fig. S2** Electron-density distribution of the highest occupied (HOMO) and lowest unoccupied frontier orbitals (LUMO) for **1**.
- Fig. S3** The ESR spectra of **1** before and after heat-treatment.
- Fig. S4** The ESR spectra of **4** before and after photoirradiation.
- Fig. S5** Total and partial density of states for **2-5**.
- Fig. S6** The view from two sides of the 2D supramolecular layer formed by alternative double helical chains in **1**.
- Fig. S7** The distance and orientation between the O⁻...N⁺ ions in **1**.
- Fig. S8** IR spectra of **1** before and after heat-treatment.
- Fig. S9** The PXRD patterns of **1**.
- Fig. S10-11** The shrink and expansion of the crystal faces in **1** after heat-treatment.
- Fig. S12-15** The IR spectra recorded for the transformation from **1** to **2-5**.
- Fig. S16-19** PXRD recorded for the bulk sample transformation from **1** to **2-5**.
- Fig. S20-23** The IR spectra recorded for the irreversible transformation from **2-5** to **1**.
- Fig. S24** The nearest distance between the O⁻...N⁺ ions in **2-5**.



Scheme S1. Carboxybenzyl-substituted viologen derivative $H_2BpybcCl_2$.

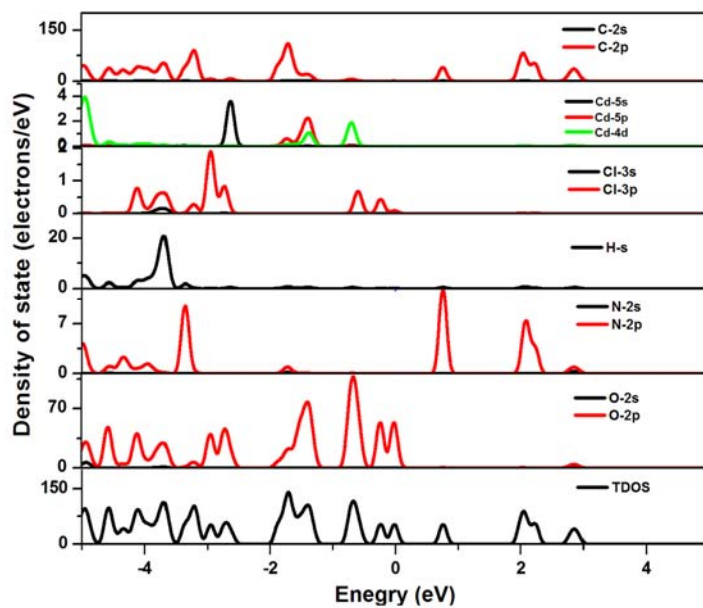


Fig. S1 Total and partial density of states for **1** (The Fermi level is set at 0 eV).

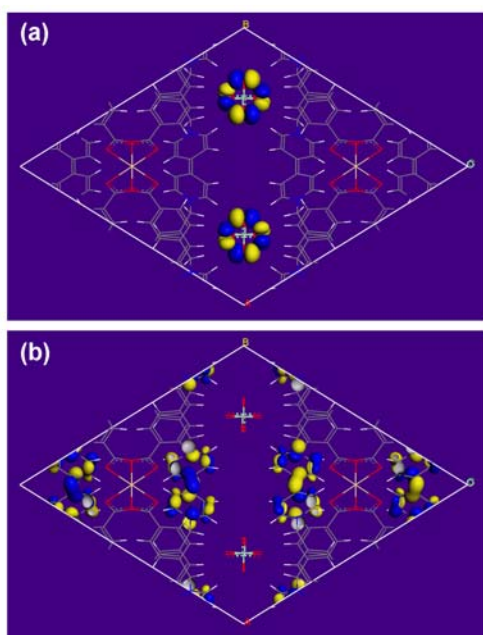


Fig. S2 Electron-density distribution of the (a) highest occupied (HOMO) and (b) lowest unoccupied frontier orbitals (LUMO) for **1**.

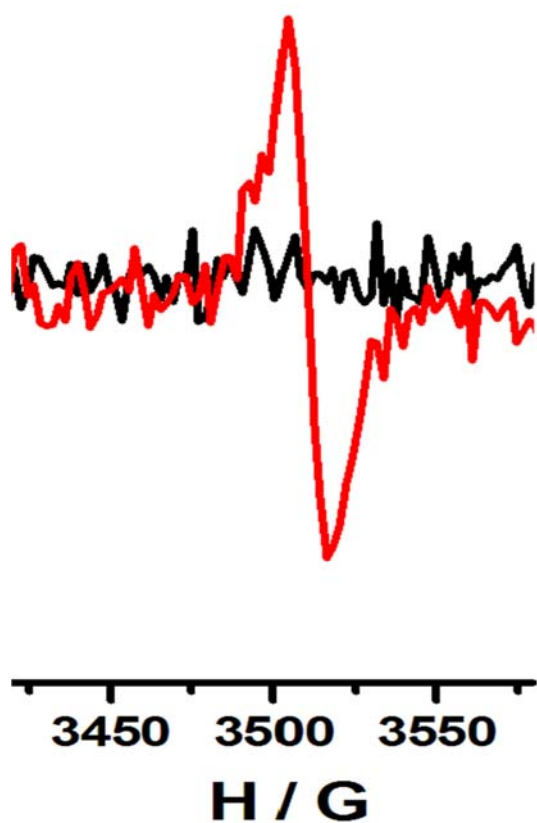


Fig. S3 The ESR spectra of 1 before (dark) and after (red) heat-treatment ($g = 2.0027$).

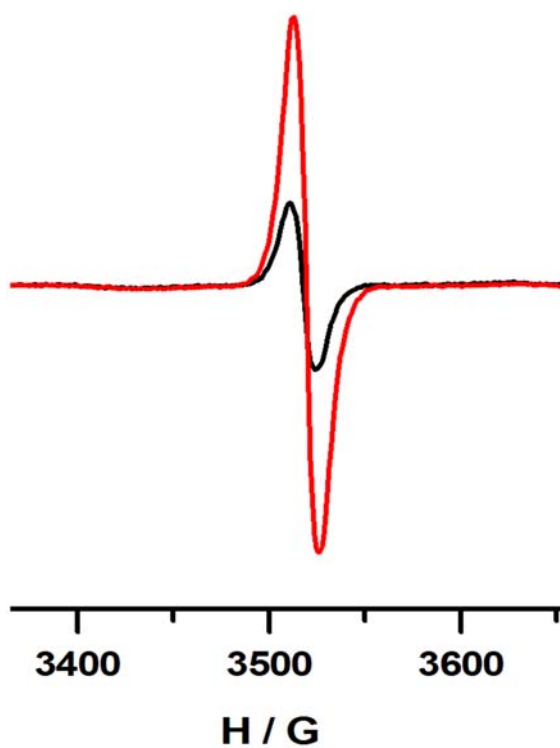


Fig. S4 The ESR spectra of 4 before (dark) and after (red) photoirradiation.

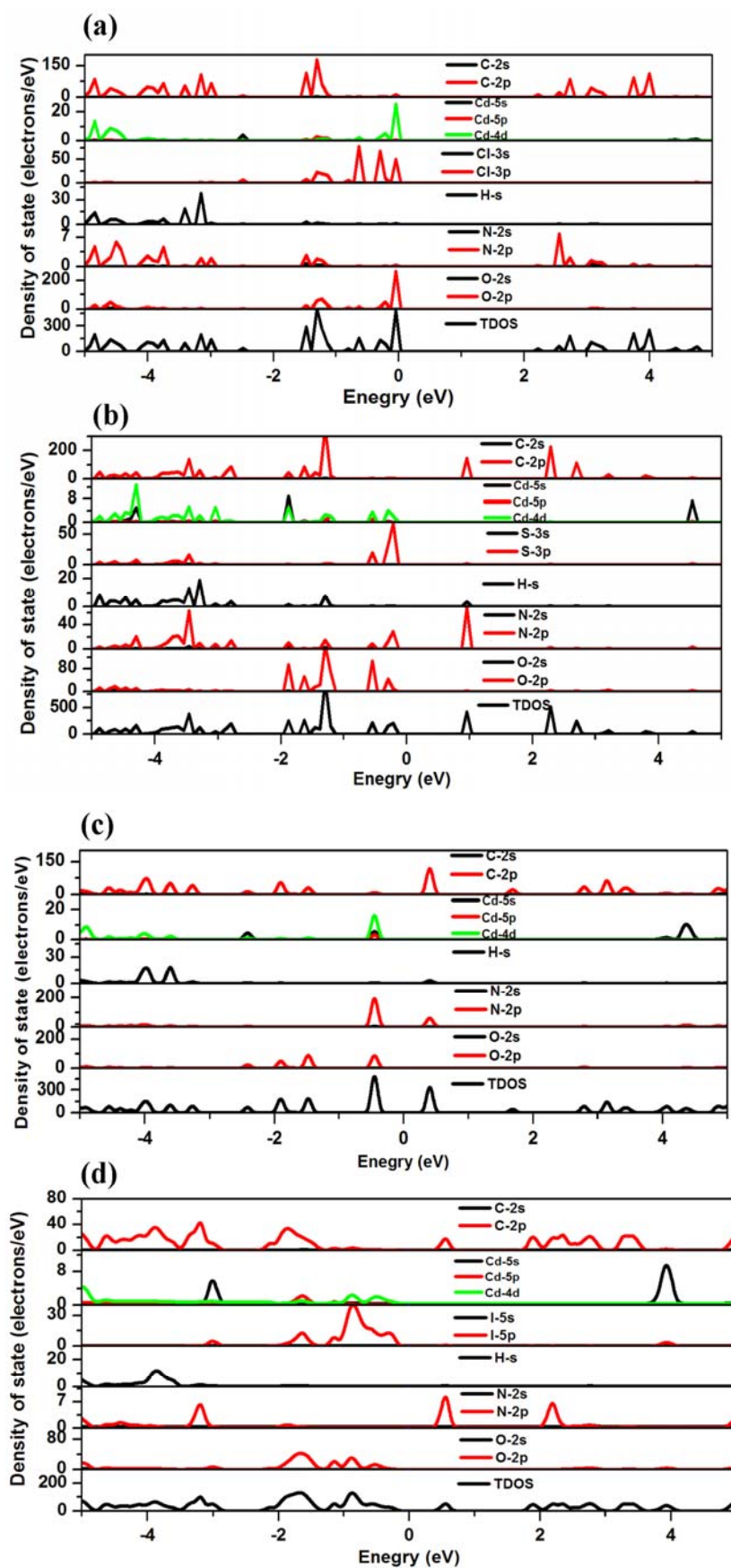


Fig. S5 Total and partial density of states for **2** (a), **3** (b), **4** (c), **5** (d). (The Fermi level is set at 0 eV).

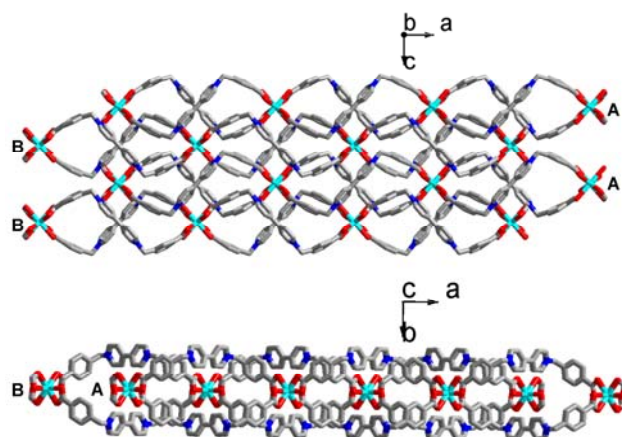


Fig. S6 The view from two sides of the 2D supramolecular layer formed by alternative double helical chains in **1**.

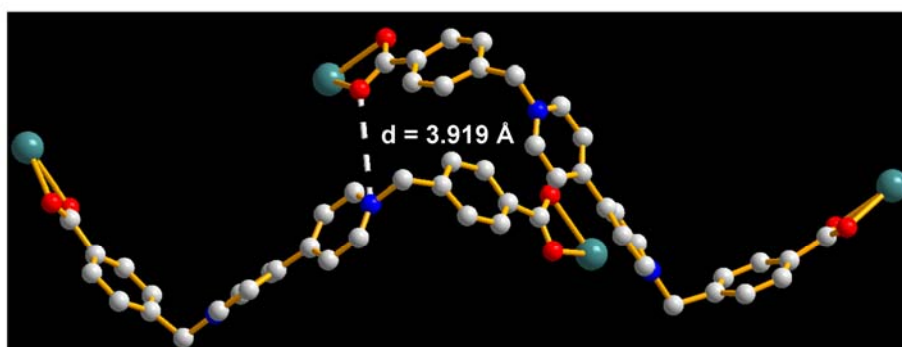


Fig. S7 The distance and orientation between the $O^- \cdots N^+$ ions in **1**. All hydrogen atoms are omitted for clarity (C grey; N blue; O red; Cd green).

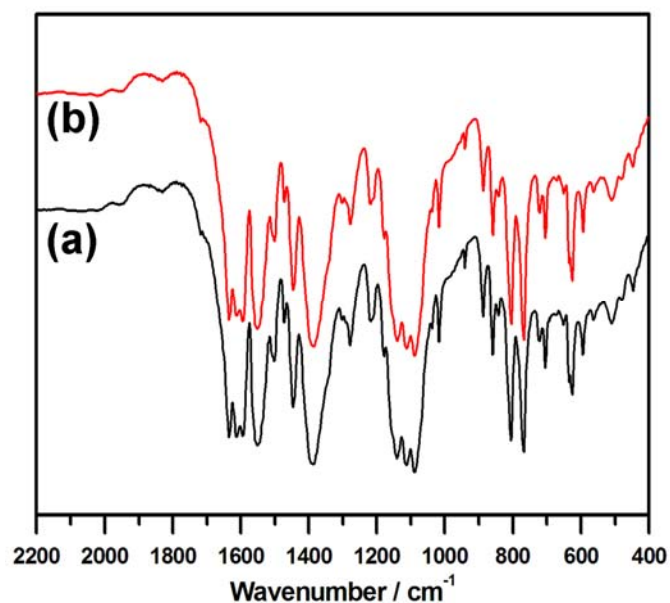


Fig. S8 IR spectra of **1** before (black) and after (red) heat-treatment. The spectra show no detectable change in band positions after heat-treatment.

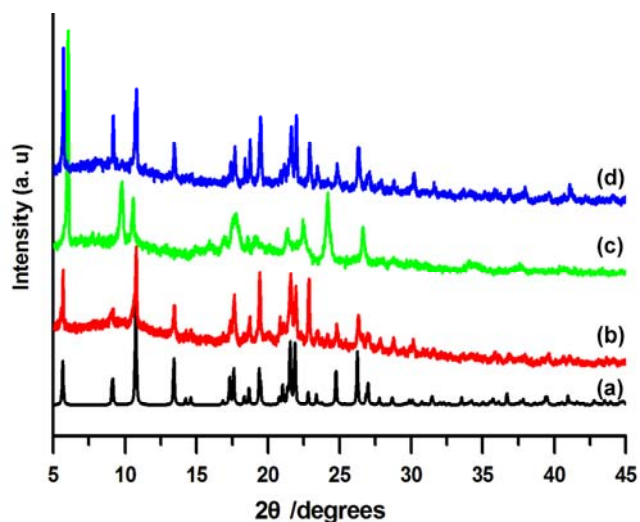


Fig. S9 The PXRD patterns of **1**: (a) stimulated, (b) as synthesized, (c) after heat-treated, (d) after standing in humid air overnight.

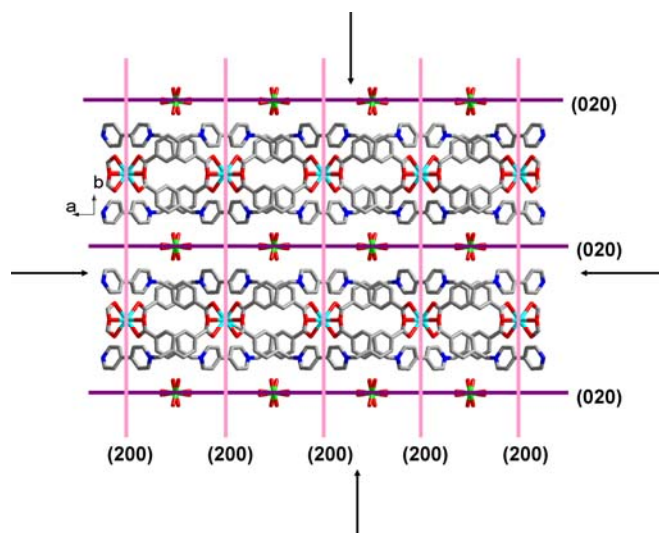


Fig. S10 The shrink corresponding to (020) and (200) crystal faces of compound **1** after heat-treatment.

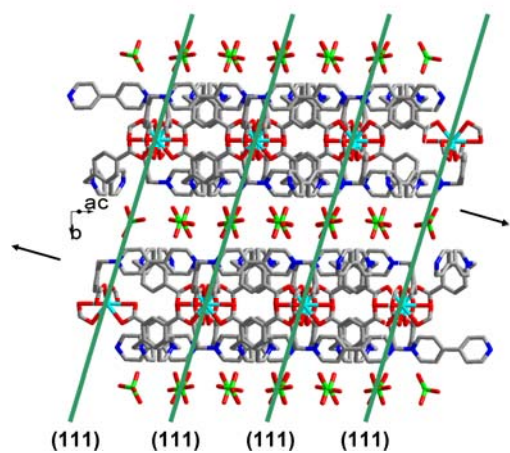


Fig. S11 The small expansion corresponding to (111) crystal faces of compound **1** after heat-treatment.

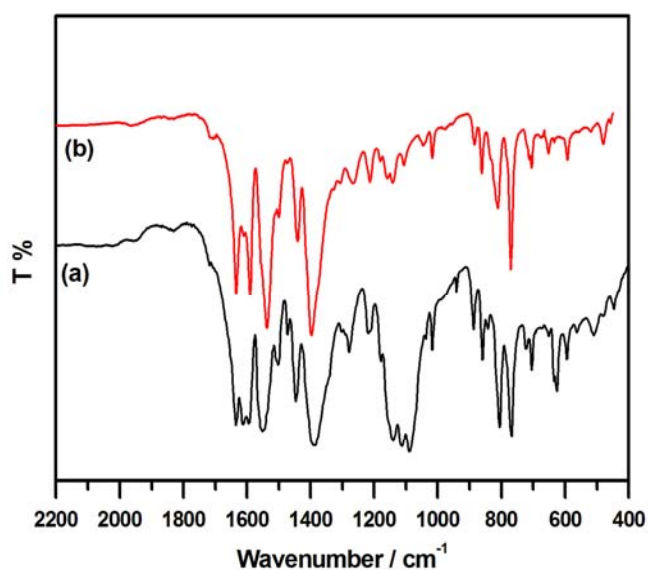


Fig. S12 The IR spectra recorded for the transformation from **1** to **2**, (a) as synthesized sample **1**, (b) after immersing **1** in 0.2 M NaCl solution for several hours. The disappearance of strong vibration bands of the ClO_4^- ion between 1080-1150 cm^{-1} demonstrates the occurrence of anion exchange process.

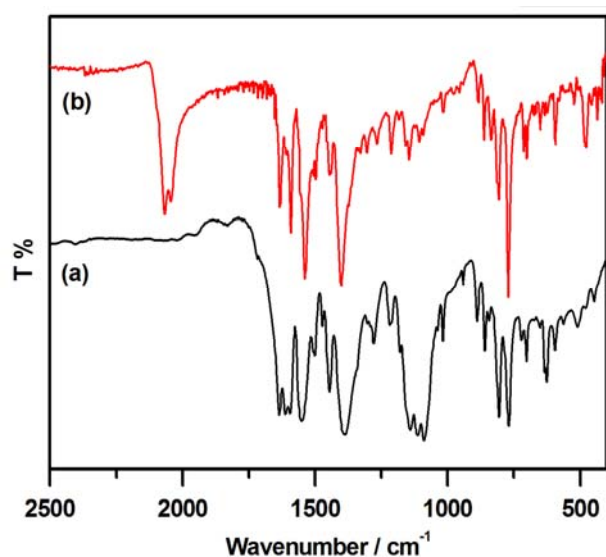


Fig. S13 The IR spectra recorded for the transformation from **1** to **3**, (a) as synthesized sample **1**, (b) after immersing **1** in 0.2 M KSCN solution for several hours. The appearance of new bands at 2069 and 2044 cm^{-1} attributed to the asymmetric stretching vibrations of the SCN^- ions is consistent with the single crystal structure analysis.

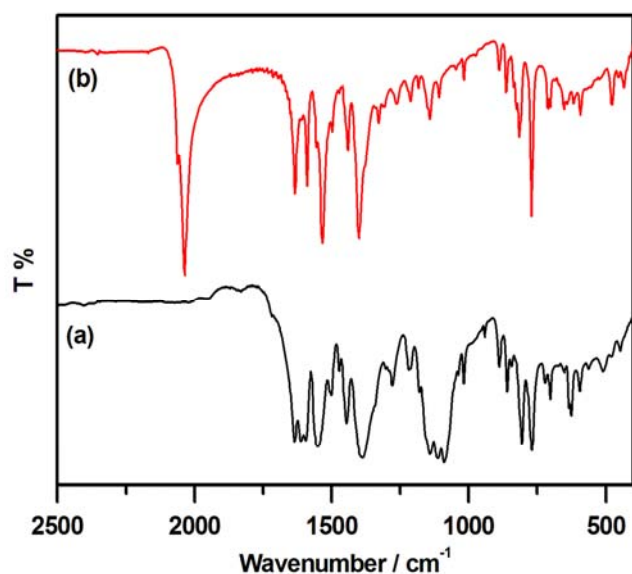


Fig. S14 The IR spectra recorded for the transformation from **1** to **4**, (a) as synthesized sample **1**, (b) after immersing **1** in 0.2 M NaN₃ solution for several hours. The appearance of new bands at 2063 and 2037 cm⁻¹ attributed to the asymmetric stretching vibrations of the N₃⁻ ions is consistent with the single crystal structure analysis.

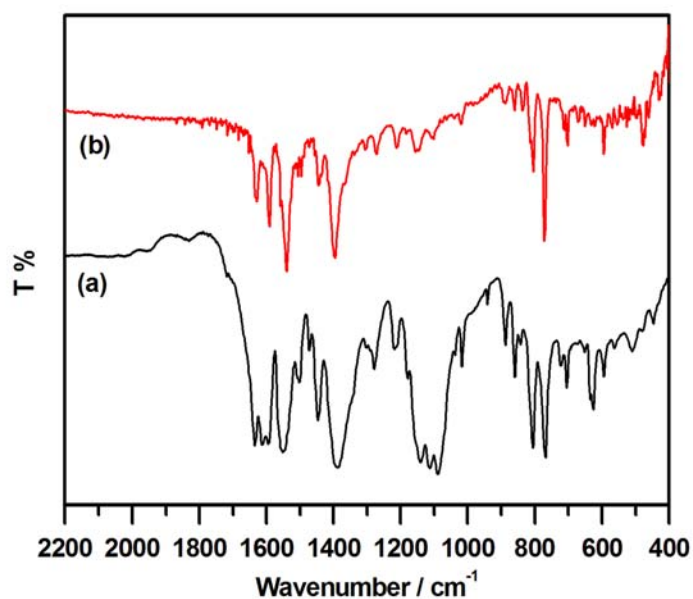


Fig. S15 The IR spectra recorded for the transformation from **1** to **5**, (a) as synthesized sample **1**, (b) after immersing **1** in 0.2 M KI solution for several hours. The disappearance of strong vibration bands of the ClO₄⁻ ion between 1080-1150 cm⁻¹ demonstrates the occurrence of anion exchange process

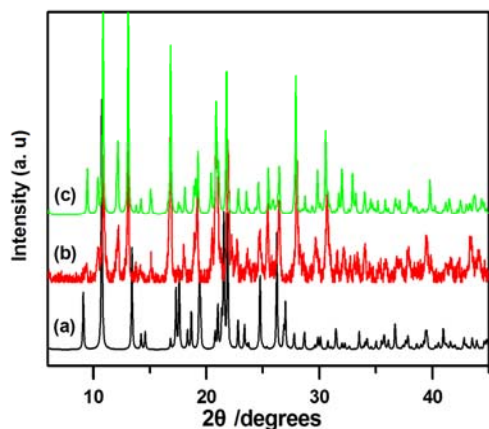


Fig. S16 PXRd recorded for the transformation from bulk sample **1** to **2**, (a) calculated pattern from single crystal **1**, (b) after immersing **1** in 0.2 M NaCl solution for several hours, (c) calculated pattern from single crystal **2**.

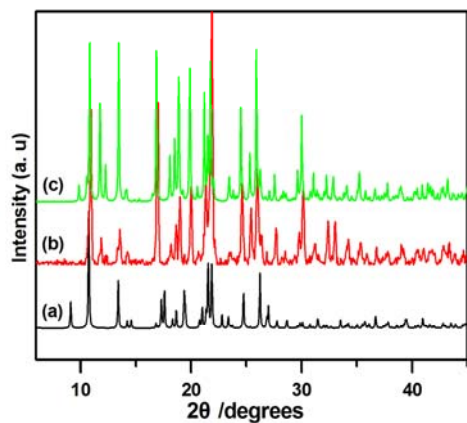


Fig. S17 PXRd recorded for the transformation from bulk sample **1** to **3**, (a) calculated pattern from single crystal **1**, (b) after immersing **1** in 0.2 M KSCN solution for several hours, (c) calculated pattern from single crystal **3**.

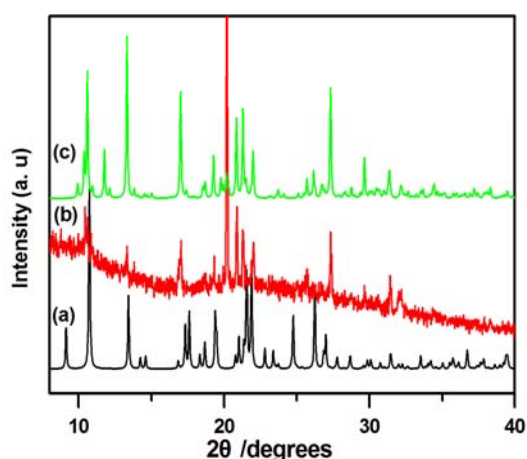


Fig. S18 PXRd recorded for the transformation from bulk sample **1** to **4**, (a) calculated pattern from single crystal **1**, (b) after immersing **1** in 0.2 M NaN_3 solution for several hours, (c) calculated pattern from single crystal **4**.

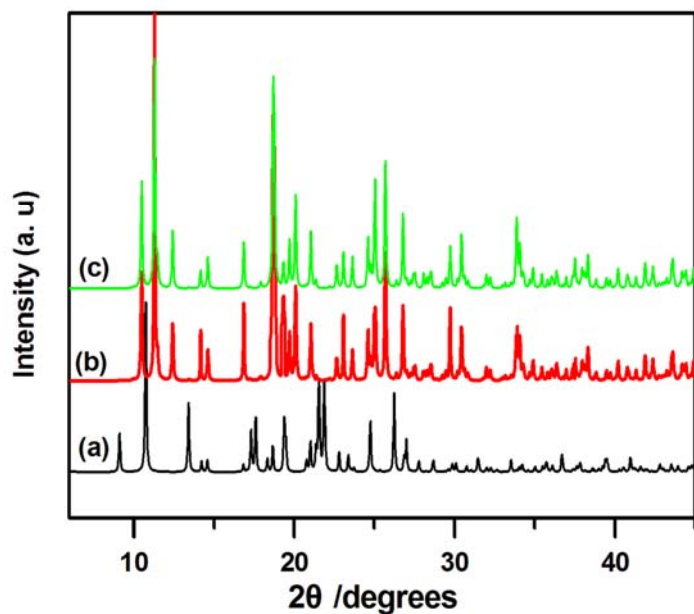


Fig. S19 PXR D recorded for the transformation from bulk sample **1** to **5**, (a) calculated pattern from single crystal **1**, (b) after immersing **1** in 0.2 M KI solution for several hours, (c) calculated pattern from single crystal **5**.

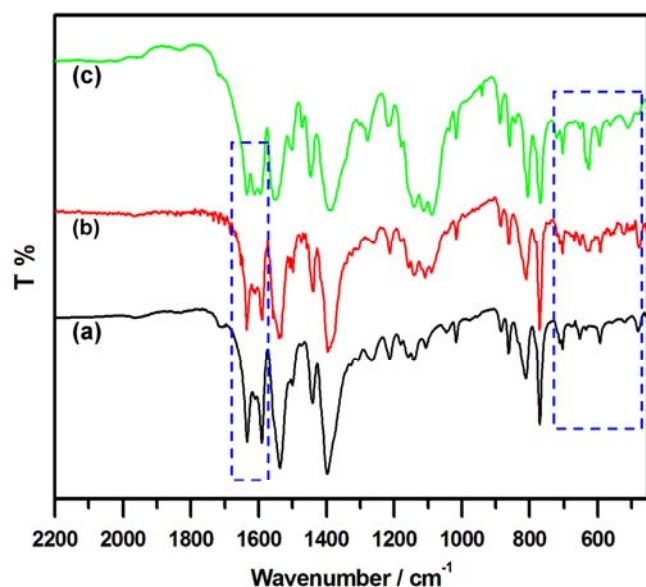


Fig. S20 The IR spectra recorded for the irreversible transformation from **2** to **1**, (a) as synthesized sample **2**, (b) sample **2'**: after immersing **2** in 0.2 M NaClO₄ solution for a week, (c) as synthesized sample **1**. The relative vibration intensity of the ClO₄⁻ ions in **2'** is weaker than that of **1**, and most of vibrations bands between 1580-1640 cm⁻¹ and in fingerprint region are still quite consistent with that **2**. Moreover, **2'** show a photochromic property, therefore we speculate that **2'** is compositionally more similar to **2**, the weak band corresponding to the vibration of ClO₄⁻ ions observed in **2'** may origin from the adsorption of the ClO₄⁻ ions on the surface of materials.

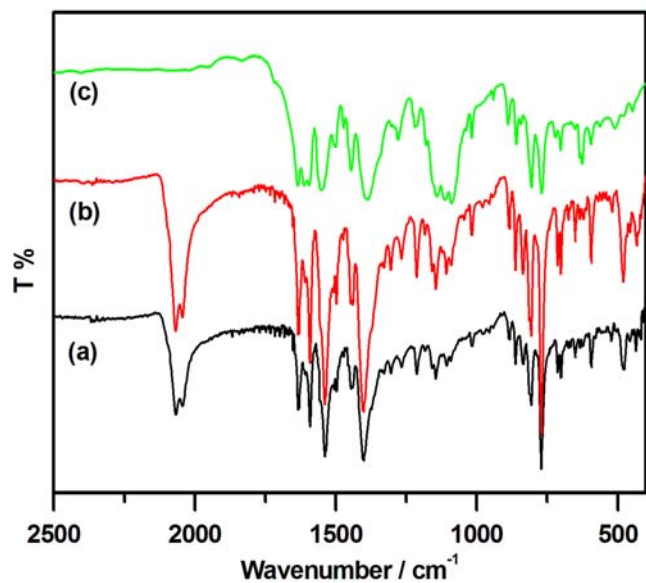


Fig. S21 The IR spectra recorded for the irreversible transformation from **3** to **1**, (a) as synthesized sample **3**, (b) after immersing **3** in 0.2 M NaClO₄ solution for a week. The almost unchanged spectra demonstrate the strong coordination propensity of terminated SCN⁻ anion, (c) as synthesized sample **1**.

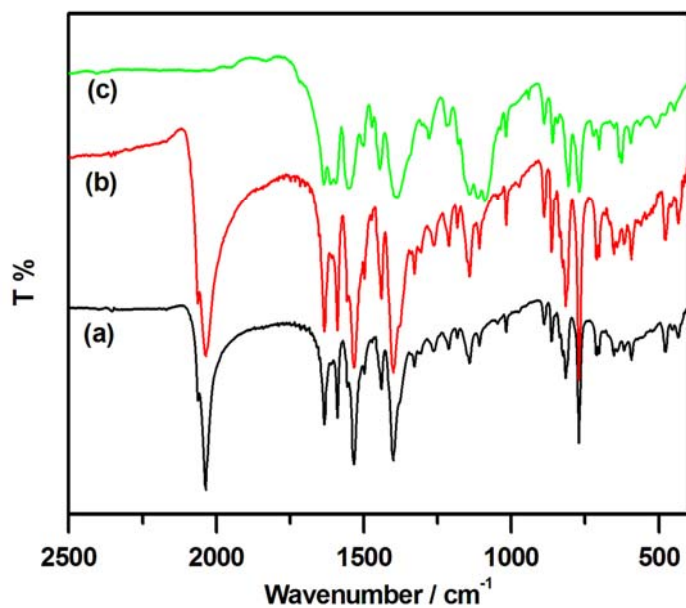


Fig. S22. The IR spectra recorded for the irreversible transformation from **4** to **1**, (a) as synthesized sample **4**, (b) after immersing **4** in 0.2 M NaClO₄ solution for a week, the almost unchanged spectra demonstrate the strong coordination propensity of terminated N₃⁻ anion, (c) as synthesized sample **1**.

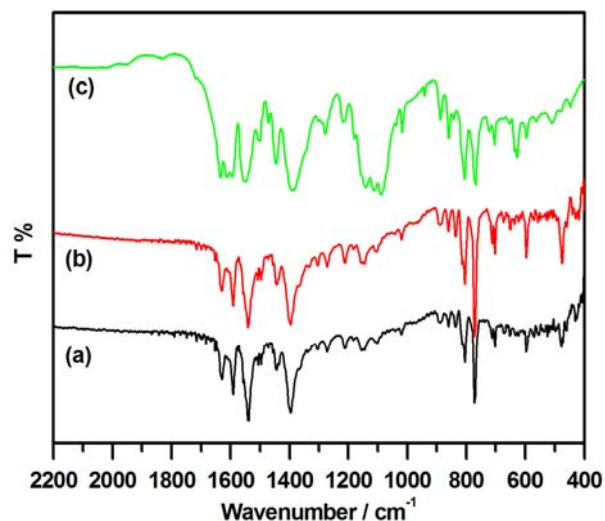


Fig. S23. The IR spectra recorded for the irreversible transformation from **5** to **1**, (a) as synthesized sample **5**, (b) after immersing **5** in 0.2 M NaClO₄ solution for a week, the almost unchanged spectra suggest that no structural transformation occurs. (c) as synthesized sample **1**.

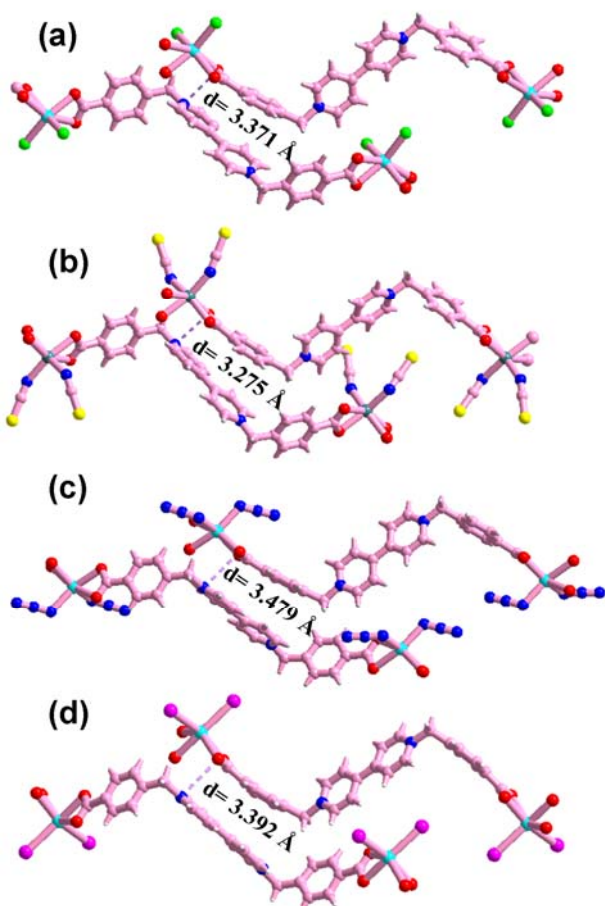


Fig. S24. The nearest distance between the O⁻...N⁺ ions in **2** (a), **3** (b), **4** (c) and **5** (d). (C rose; N blue; O red; Cd turquoise; Cl bright green; S yellow; I pink; H gray).